

A MWPC WITH A CATHODE COUPLED DELAY LINE READ-OUT AS RADIOACTIVITY DETECTOR FOR DNA REPAIR STUDIES

R. BELLAZZINI, A. DEL GUERRA, M.M. MASSAI, M. RAGADINI, G. SPANDRE and G. TONELLI

Istituto di Fisica dell'Università, Piazza Torricelli 2, I-56100 Pisa, Italy

INFN - Istituto Nazionale di Fisica Nucleare, Sezione di Pisa, San Piero a Grado, Via Livornese, I-56010 Pisa, Italy

Received 19 December 1980 and in revised form 26 June 1981

A non selective method for the isolation of DNA repair-deficient mutants in mammalian cells is discussed. The method requires radioactive labelling of the short DNA sequences synthesized during repair of damaged regions. Mutants should be recognized by the absence of radioactive incorporation into their DNA. A multiwire proportional chamber (MWPC) is proposed as a suitable radioactivity detector. The performance of a MWPC prototype with a cathode coupled delay line read-out is described and is shown to be adequate for this application. The main advantages of a MWPC are reviewed with respect to other methods used for β^- radioactivity counting of biological samples, such as liquid scintillators or autoradiography: the proposed detection method is non destructive for the cells, which are being kept alive for further biological studies; furthermore many cell clones can be screened within a reasonable time.

1. Introduction

Under the expression "DNA repair", a large variety of complex biological processes are included. They all aim at the restoration of the normal structure of DNA, the polymeric molecule carrying the genetic information, whenever it is changed by endogenous or exogenous factors.

The possibility of studying the biochemistry and the genetics of DNA repair largely depends on the availability of mutants lacking the ability of performing specific enzymatic steps of the repair pathways. In fact, more is known at present on the repair mechanisms of bacteria than of mammals, because repair-deficient mutants can easily be induced and isolated in microorganism but not in higher organisms.

Although the temptation exists simply to extrapolate to mammalian cells our knowledge about bacteria, one has to realize that major differences might exist in the repair mechanism of DNA in different organisms. Eukaryotic cells (mammalian cells, for example) have a highly organized structure for their DNA, which involves the association of DNA with proteins and the coiling of DNA-protein particles, according to regular, specific patterns. Such a complex organization of genetic material is not present in chromosome of prokaryotes, which bacteria belong to. The genetic control of DNA replication,

to which DNA repair is coupled, is also different in eukaryotic and prokaryotic organisms. For these differences, we can assume that the two classes of organisms also deal in different ways with damage in their DNA.

Our knowledge of DNA repair in mammalian cells is at present rather rudimentary. It is mainly based on the study of a small number of human diseases associated with defective DNA repair. In 1968, it was discovered [1] that individuals affected by the genetic disease xeroderma pigmentosum, who suffer from skin cancer when exposed to sunlight, are characterized by the fact that their cells are unable to repair DNA damage induced by ultraviolet light. This finding has stimulated the search for other human "mutants" showing an association between defective DNA repair and a higher propensity for cancer. Several cases have indeed been found [2].

Human diseases, however, most probably represent only a selected sample of all possible defects in DNA repair. By this approach, therefore, our attempts to understand the basic mechanism of DNA repair in man and other mammals will remain severely limited.

An alternative possibility is to artificially induce DNA repair mutants in mammalian cells cultured "in vitro". A broader spectrum of genetic defects should then be obtained, which will enable the

identification of a higher number of the biochemical steps involved in the repair processes. The main difficulty with this approach is the lack of a suitable method for the identification of the mutants, once they have been induced in a cell population. Methods proved successful in bacteria, such as the classical "replica plating" used for the selection of UV-sensitive clones, are not readily applicable to cultured mammalian cells. Direct screening without selection, on the other hand, which would imply testing of individual cells or clones for their capacity of repairing DNA damages, is in general not feasible because of the low frequency at which mutants occur.

If selective techniques are excluded, a method for detecting repair deficient mutants should combine both a relevant and easily recognizable change in cell phenotype, and a rapid, possibly automatic screening of cells or clones for that phenotype.

Most of the known repair mechanisms involve the unscheduled synthesis of short DNA sequences which will replace the damaged regions. As a consequence, repair-deficient mutants may be recognized by their inability to incorporate a radioactive precursor in their DNA in conditions in which repair should normally occur [3]. The use of this mutant phenotype requires suppression of scheduled DNA synthesis, which takes place when cells are duplicating their genetic material. Moreover, conditions should be sought in which radioactive molecules not incorporated into DNA are excreted. Both these requirements can be fulfilled through the use of appropriate techniques, as explained below.

The general outline of a typical experiment is the following: cells of human origin from a healthy culture are seeded into petri dishes in the presence of nutrient medium. In due time, they become attached to the bottom of this dish and start to proliferate, resulting in discrete, visible cell aggregates or "colonies". Media and glassware for mammalian cell cultures have been described elsewhere [4].

Hydroxyurea, a substance which specifically inhibits DNA replication but not repair synthesis [5], is added to the cultured colonies which are then exposed to 2600 Å UV light, at an energy flux of the order of 5 J/m². A radioactive precursor of DNA synthesis, such as ¹⁴C-thymidine, is added to the culture and, after an appropriate labelling time, the residual ¹⁴C-thymidine not used for DNA synthesis is washed out by chasing with a one-thousand fold excess of cold thymidine. By this procedure

only the radioactivity bound to macromolecules will remain within the cells.

Since DNA replication is blocked by the inhibitor, the radioactive precursor will mainly be utilized by the cells engaged in the repair of DNA sequences damaged by the UV-treatment. As a result, repair-competent colonies will incorporate radioactivity, whereas repair-deficient mutants will stay unlabelled. We are then left with the problem of distinguishing rare unlabelled colonies interspersed with a great majority of labelled colonies.

As for the radioactivity counting, the method of choice must be non destructive for the cells, since the whole procedure aims at the isolation of mutants to be used for further biological study. The method should also have high spatial resolution, high sensitivity and low time-consumption.

Two methods are commonly used in radiodensity analysis:

- (i) liquid organic scintillator technique
- (ii) autoradiography with emulsion.

Both of them do not seem appropriate to this biological application. The first method, in fact, would require all the colonies to be measured one by one. Too long a time is then necessary for the analysis in order to achieve the required statistics; furthermore, this measurement is fully destructive for the colonies. As for the second method, the time necessary for each autoradiography is also prohibitively long (several days), because of the intrinsic low sensitivity of this technique, and the cells do not stay alive at room temperature for such a long time.

In this paper a multiwire proportional chamber (MWPC) is proposed as a more suitable detector. The performance of a MWPC prototype constructed for such an application is presented in section 2. The cathode coupled delay line read-out system is fully described in section 3 and the measured spatial resolution in section 4. Finally the overall performance of the MWPC is discussed and is shown to be adequate for the described biological application.

2. The MWPC and its performance

The constructed MWPC prototype is mostly standard (6) in terms of mechanics and gas filling.

A cross view of the prototype is shown in fig. 1a. The chamber is made of six fiber-glass frames; the outer frames are 16 mm thick and the inner ones 6 mm. The active area is 250 × 250 mm² and the

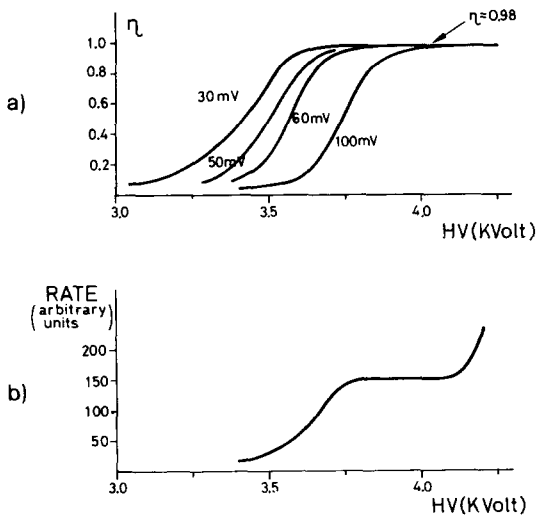


Fig. 3. Typical plateau curves for minimum ionizing particles: a) efficiency at various thresholds, b) singles rate at a threshold of 100 mV. The gain of the amplifier was set at 250.

than 400 V has been obtained in the working range of threshold (i.e. 30–60 mV). Fig. 3b shows a typical distribution of the singles rate of the chamber versus the voltage at a threshold of 100 mV. Fig. 4a shows

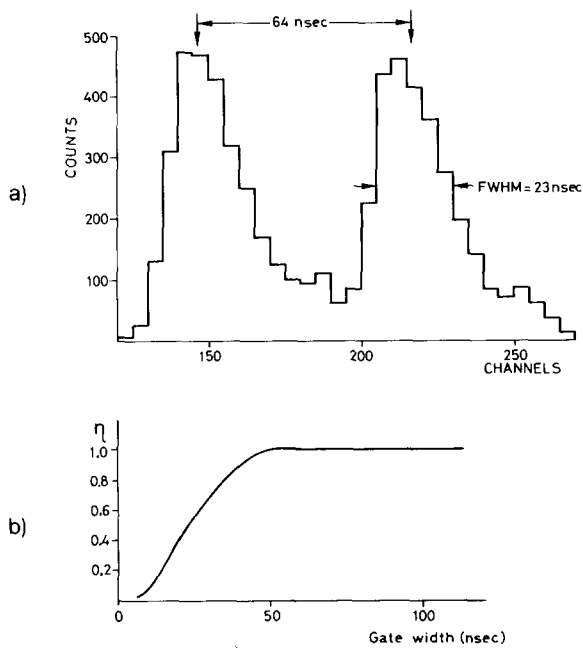


Fig. 4. a) Time distribution of the charge collection for minimum ionizing particles; the two spectra differ by a 64 ns external delay (see text); b) efficiency as a function of the gate width of the trigger–MWPC coincidence.

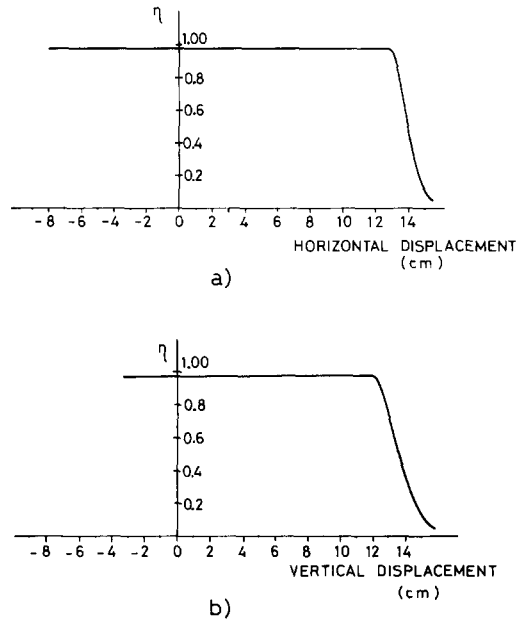


Fig. 5. Typical uniformity plots for: a) a horizontal scan, b) a vertical scan.

the time distribution of the avalanche collection on the anode wire. To self-calibrate the distribution a second spectrum is plotted on the same figure,

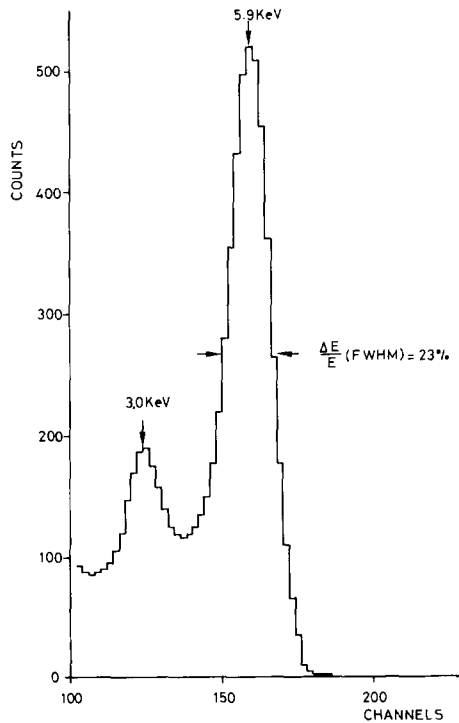


Fig. 6. Energy resolution spectrum with ⁵⁵Fe X-rays at the anode voltage of 3.5 kV.

obtained by simply adding a fixed delay of 64 ns to the anode signal. The fwhm of these spectra is ~ 23 ns. It is evident from fig. 4b that a gate width of 50 ns is long enough to ensure the collection on the anode wires of all the primary ionization. Good uniformity of the MWPC response has been measured across the active area. This is illustrated in fig. 5, where the efficiency for m.i.p. is shown as a function of the displacement of the chamber relative to the narrow beam as defined by the trigger. Fig. 6 shows the energy resolution of the MWPC irradiated by a ^{55}Fe source (5.9 keV X-rays), when the anode signal is given by a single wire. The presence of the 3.0 keV "escape peak" of the argon fluorescence X-ray, together with the 5.9 keV photopeak is a convenient way to self-calibrate the spectrum [7]. A $\Delta E/E$ of 23% (fwhm) has been measured at 3.5 kV of applied anode voltage.

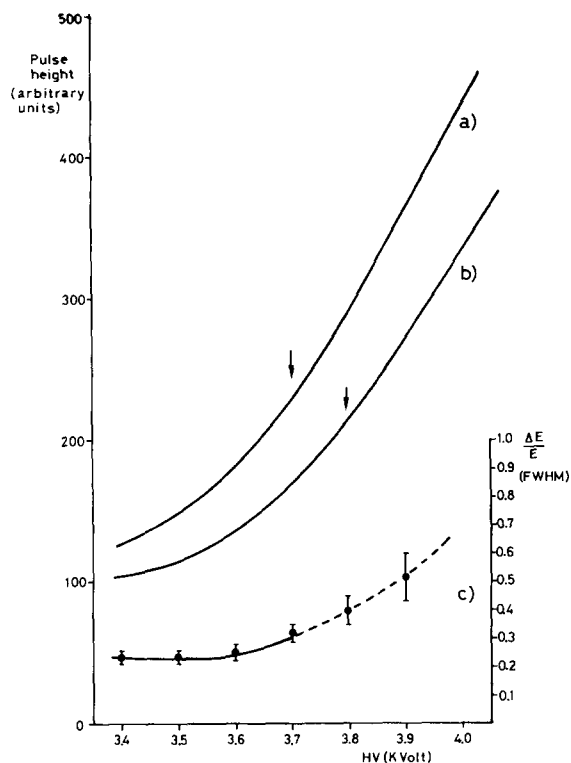


Fig. 7. Pulse height dependence on applied voltage with ^{55}Fe X-rays when the anode signal is given by a single wire. Curves a) and b) refer to the full energy peak (5.9 keV) and to the escape peak (3.0 keV), respectively; the arrows show the beginning of the semiproportional region. The energy resolution data at 5.9 keV are also plotted in the same figure on a different scale; the solid-dashed line is a hand drawn fit to the data; the dashed part spans the semiproportional region.

Finally, the $\Delta E/E$ values (fwhm) at 5.9 keV as a function of the applied voltage is shown in fig. 7, together with the channel positions of the full-energy and of the escape peak in the corresponding energy spectra. The energy resolution worsens with increasing voltage, because the chamber working condition moves from proportional to semiproportional region.

3. The delay line read-out system

3.1. The cathode read-out

When a negative charge $-Q$ is released on the anode wire by the positive receding ions cloud, a positive charge $+Q$ is globally induced on the surrounding electrodes, i.e. the other anode wires and the facing cathode wires. Due to the electric field configuration, the signal induced on the cathode plane is spread out in a discrete way among several wires [7,8]. By a capacitive coupling, it is possible to transfer these smoothly distributed cathode signals to a continuous delay line [9–11]; the measurement of the time of arrival of the signal centroid at the end of the delay line can be related to the original positive charge distribution on the cathode wires and then to the position of the primary ionization event in the chamber. With this read-out system one can measure the position along the anode wire to an accuracy better than the wire spacing. Furthermore, the total cost of the electronics is kept reasonably low as opposed to a wire-per-wire read-out system. Three channels are indeed sufficient for two dimensional read-out: one START (the anode signal) and two STOP (the two delay lines output signals).

3.2. The delay line

To obtain a suitable spatial resolution on the entire chamber, the delay line must satisfy the following specifications:

- the capacitive coupling coefficient must be high, especially if the MWPC has to work in the proportional region, i.e. at low gain;
- the phase dispersion must be kept low in the useful frequency range as covered by the induced signal;
- the time delay per unit length has to be high enough to allow the required spatial resolution.

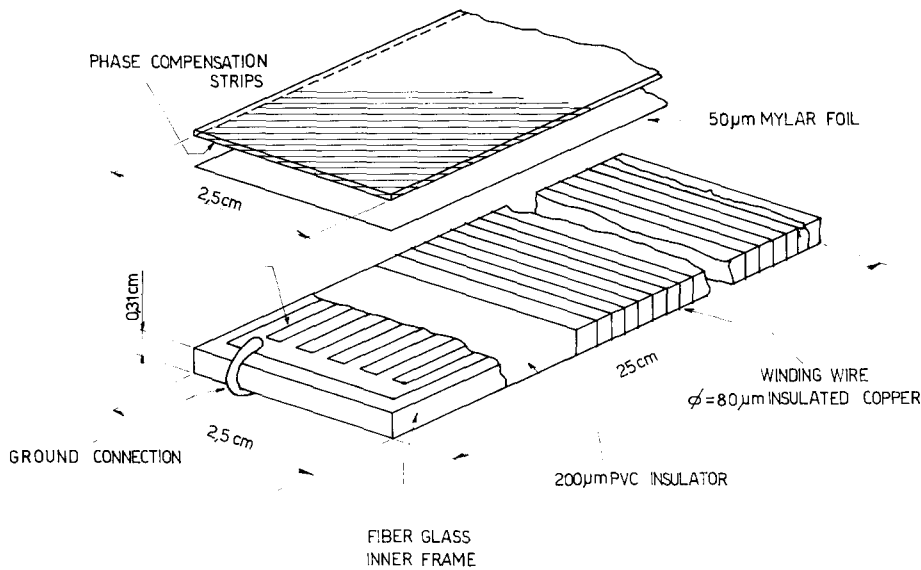


Fig. 8. Exploded view of the delay line and of the floating patch (figure not to scale).

The construction details of the delay line are shown in fig. 8. Its core is a fiberglass board, as used for printed circuits; several longitudinal copper strips have been impressed on the board as ground reference for the signal. The core is surrounded by a dielectric sheath (thermoretractile PVC), which determines the capacity of the delay line. An insulated copper wire ($\phi = 80 \mu\text{m}$) is wound around it with a $90 \mu\text{m}$ pitch. The large transversal dimension of the delay line (2.5 cm) and the high characteristic impedance (1750Ω) enable to achieve a good coupling to the cathode signal. The main characteristics of the delay line are presented in table 1.

3.3. Performance of the delay line

Since the time delay per unit length, τ_1 , is proportional to $\sqrt{L_1 C_1}$ (where L_1 and C_1 are the inductance

Table 1
Delay line characteristics

Width	2.5 cm
Length	20 cm
Thickness	0.31 cm
Diameter of the copper winding wire	80 μm
R (ohmic resistance)	$(380 \pm 5) \Omega$
Z_0 (characteristic impedance)	$(1750 \pm 50) \Omega$
Total delay	880 ns
Delay per unit length (τ_1)	44 ns/cm

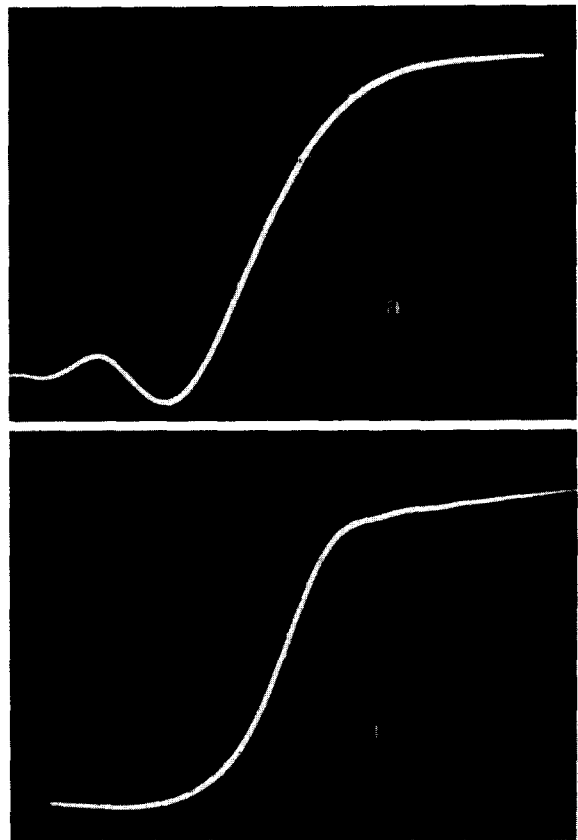


Fig. 9. Typical output responses to input signals directly fed into the delay line: a) without compensation strips, b) with compensation strips. Horizontal scale is 100 ns/div.

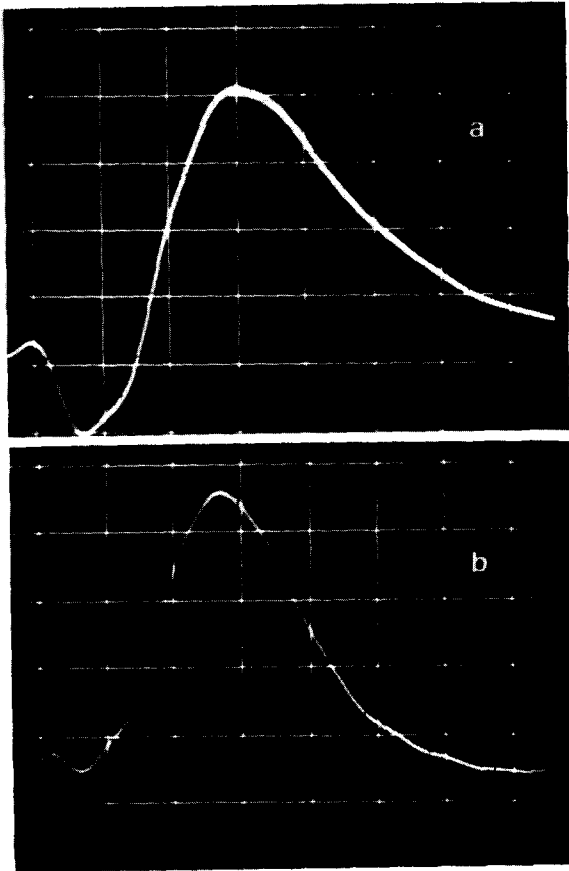


Fig. 10. Typical output responses of the delay line to capacitively induced input signals: a) without compensation strips, b) with compensation strips. Horizontal scale is 50 ns/div.

and the capacitance per unit length, respectively) and L_1 is a decreasing function with frequency, τ_1 decreases with increasing frequency. Such a dependence causes a strong phase distortion in the output signal as shown in figs. 9a and 10a.

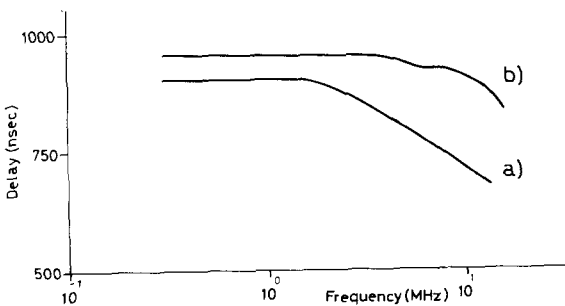


Fig. 11. Dependence of the total delay on the signal frequency: curves a) and b) refer to the unpatched and patched delay line, respectively.

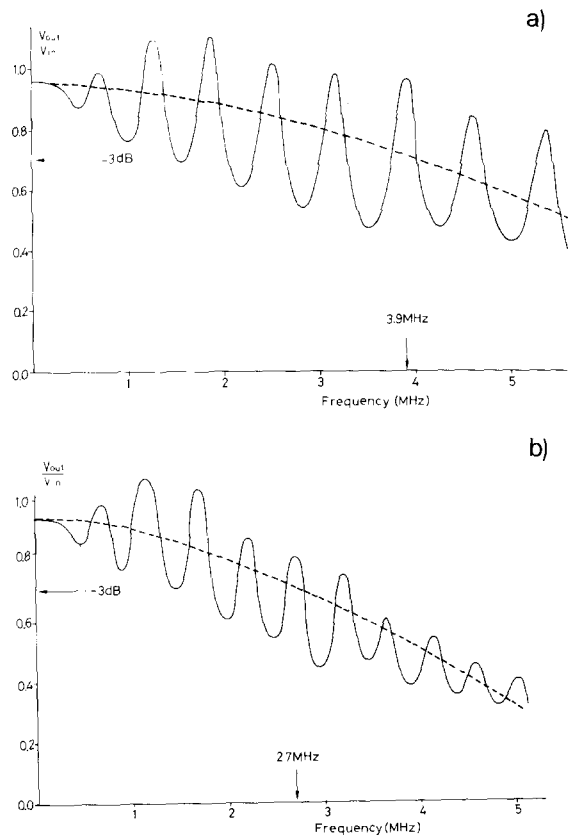


Fig. 12. V_{OUT}/V_{IN} ratio versus frequency for the: a) unpatched, b) patched delay line. The dotted line is drawn by eye to show the average value of that ratio.

In order to minimize this effect, the capacitance seen by the signal which propagates along the delay line must increase with frequency in such a way as to keep τ_1 roughly constant. In practice, this compensation effect can be obtained with the technique of “floating patch” [9–11], as originally proposed by Kallmann [12]. Several copper strips (0.5 mm width, 0.5 mm apart) are impressed on a printed circuit board of the same size of the delay line. The strips are inclined at 45° , which is the angle that experimentally optimizes the results. The floating patch is then placed on the outer face of the delay line, with a $50 \mu\text{m}$ Mylar foil in between (fig. 8). The effect of the compensation strips on the output signal is clearly shown in figs. 9b and 10b.

The total delay as a function of frequency is shown in fig. 11. The curves a) and b) refer to the delay line without and with compensation strips, respectively. It is worth pointing out that the floating patch increases the specific delay (by 10%)

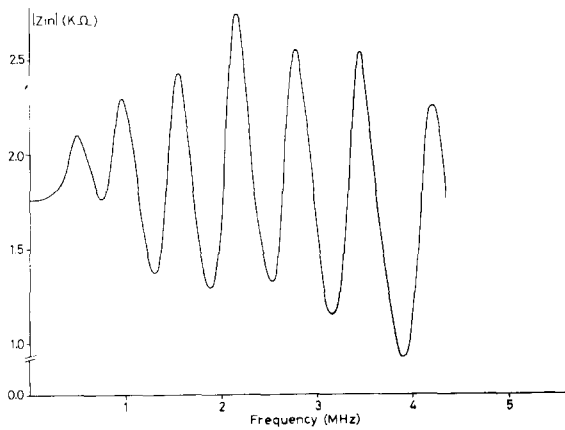


Fig. 13. Dependence of the input impedance ($|Z_{IN}|$) on the signal frequency.

and improves the rise time of the signal of about 30%.

Because of the complex impedance of the delay line, the signal attenuation depends on the frequency. Such a dependence is usually given in terms of the bandwidth, i.e. the frequency value at which $\log_{10}(V_{OUT}/V_{IN}) = -3$ db, where V_{OUT} and V_{IN} are the output and input signal, respectively. The ratio V_{OUT}/V_{IN} as a function of frequency is shown in fig. 12a and Fig. 12b for the unpatched and the patched delay line, respectively; V_{IN} was a pure sinusoidal signal directly fed into one extremity of the delay line and V_{OUT} was measured at the other extremity, terminated on its characteristics impedance at low frequency (Z_0). The input impedance of the delay line, Z_{IN} , depends on the signal frequency with the characteristic oscillatory behaviour as shown in fig. 13, and tends asymptotically to the

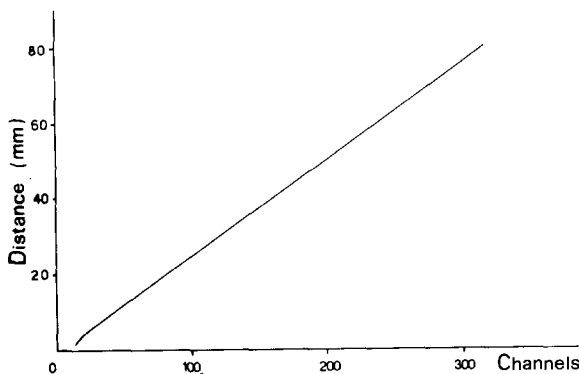


Fig. 14. Delay line linearity.

low frequency value Z_0 . Due to this mismatch the ratio V_{OUT}/V_{IN} oscillates as a function of frequency (and in opposite phase to Z_{IN}), as is clearly shown in fig. 12a and 12b. By adding a new frequency dependent capacitance, the oscillations are reduced at high frequency (i.e. the floating patch equalizes the specific delay) and the band-width does not decrease very much (from 3.9 MHz to 2.7 MHz). The distance in frequency between two consecutive maxima in the oscillations (Δf_i) is related to the specific delay at the i th frequency (T_i) by the expression $\Delta f_i \approx 1/2T_i$, as already pointed out by Kallmann [12].

The delay line linearity was tested by directly sending a signal from a pulse generator to the cathode wires and measuring the induced signal at one end of the delay line. No loss of linearity has been observed except very close (a few cathode strips) to both ends of the delay line (fig. 14), where there is a significant change in the specific mutual inductance.

4. Spatial resolution of the chamber

4.1. The intrinsic resolution of the read-out system

The contribution of the electronic noise to the spatial resolution was measured by sending a positive signal from a pulse generator directly to an anode wire (Fig. 15a). Signals of the same sign are then capacitively induced on the cathode wires. The generator setting is chosen in such a way as to produce cathode signals with the same features (risetime, amplitude, etc...) as those produced by a ^{55}Fe source. The same signal from the pulse generator is also sent to the START of a time-to-amplitude converter (TAC). The output signal from the delay line (90° to the anode wires) is sent to an emitter follower (EF) for impedance matching, to a timing filter amplifier (TFA—ORTEC 454) to a constant fraction discriminator (CFD—ORTEC 437A) operating in the external mode and to the STOP of the TAC. The differential and integral shaping constants of the TFA optimize the signal to noise ratio and equalize the output signal waveform for input signals that have been induced at different position along the delay line and, therefore, have a different rise time, as discussed in section 3.3. With the C.F. technique [13] time walk due to the rise time and amplitude variations of the input signals is minimized by proper selection of a shaping delay time; jitter is also minimized by proper selection of the attenuation factor

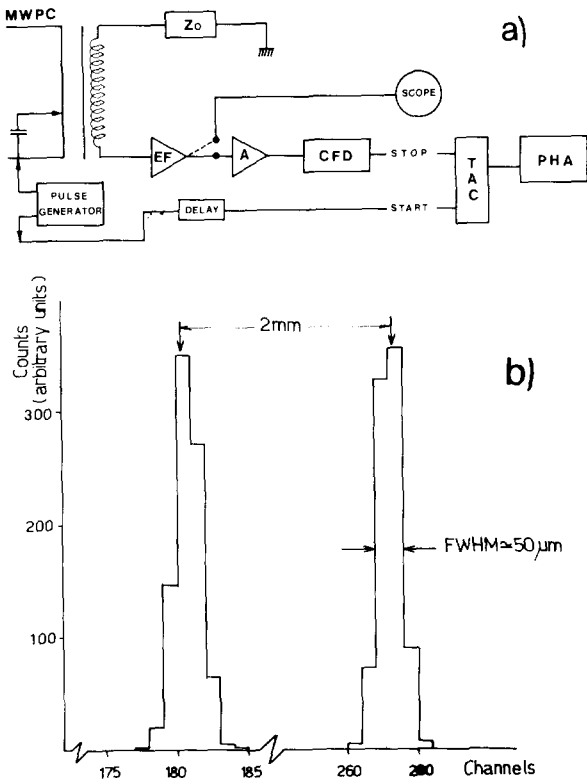


Fig. 15. Intrinsic spatial resolution measurement: a) electronic set-up, b) typical time distribution for two anode wires spaced by 2 mm.

that determines the triggering fraction.

The arrival time distribution from two adjacent anode wires (2 mm spaced) is shown in fig. 15b. The fwhm is $\sim 50 \mu\text{m}$.

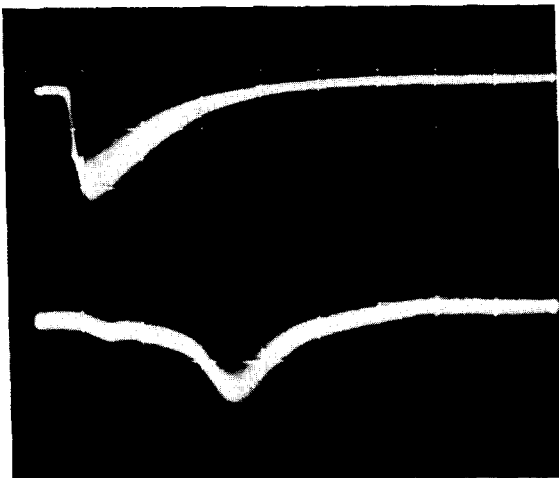


Fig. 16. Delay line output (lower) signal triggered by the anode (upper) signal. The delay line signal is shown with reversed polarity. Horizontal scale is 100 ns/div.

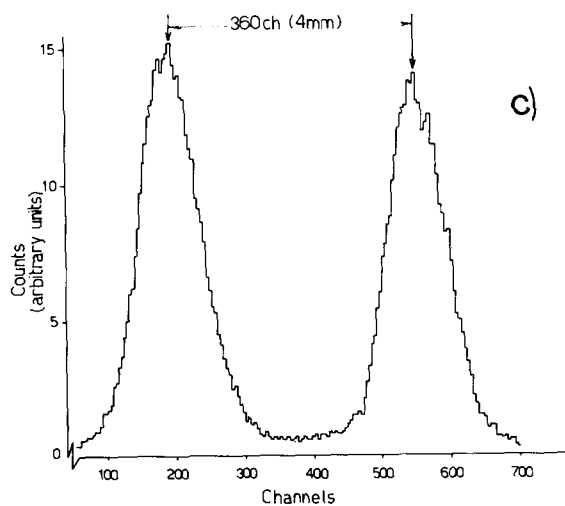
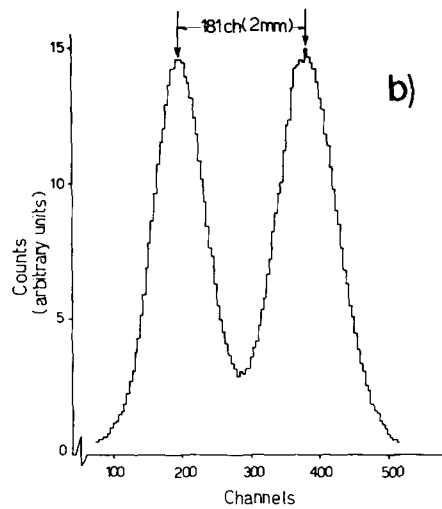
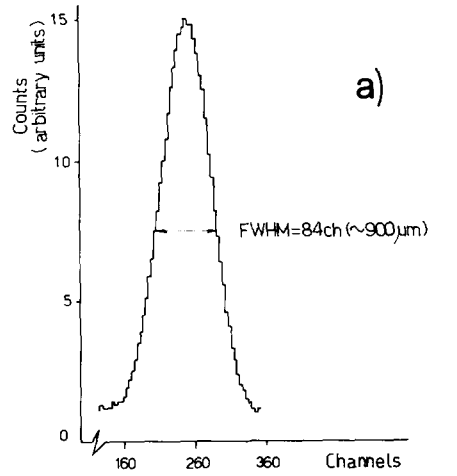


Fig. 17. Spatial resolution as measured with a ^{55}Fe source (see text).

4.2. Spatial resolution with ^{55}Fe X-rays

The spatial resolution was measured with the delay line 90° to the anode wires, by using a ^{55}Fe source. In this configuration the ultimate spatial resolution of the system can be measured; the source may be considered localized on the anode wire and the problem related to the finite dimensions and to the collimation of the source may be neglected [14]. Figs. 16 shows a typical anode signal and the corresponding delay line output signal.

The electronic read-out scheme is very similar to that of fig. 15a; in this case the START is given by the anode signal. Fig. 17 shows the arrival time distribution of the delay line output signal when the system is triggered by: a) one anode wire, b) two anode wires (2 mm spaced), c) two anode wires (4 mm spaced). The fwhm of these distribution is ~ 900 μm .

5. Discussion

In the previous sections we have described the overall performance of the MWPC prototype, and in particular the read-out system adopted. Before using the chamber as β^- radioactivity detector in the proposed biological application, three "parameters" must be discussed in detail: spatial resolution, total time necessary to perform the whole experiment, sensitivity of the chamber to low level β^- radioactivity.

As outlined in section 1, the radiodensity of aggregates of living cells (colonies) has to be measured. The dimension of each colony is determined by the growing time of the cell culture, whereas the mean separation between two colonies depends upon the cell concentration in the nutrient medium in which the cells were at random diluted. Typical values of 0.1–0.3 cm for the colony diameter and an average spacing of 0.3–0.5 cm between colonies have been obtained [15]. The measured spatial reso-

lution of the MWPC (900 μm fwhm) is then good enough to avoid topological superimposition in the reconstructed map of radioactivity.

The frequency at which mutants spontaneously appear in mammalian cells is very hard to estimate, but is far too low for this kind of experiment. It is possible, however, to increase the mutants frequency, by adding chemical mutagenic agents (typically alkylating agents) to the originally "healthy" culture of cells. By this procedure, we expect to obtain an overall (mostly induced) mutants frequency of the order of 10^{-4} – 10^{-6} . The total number of colonies we have to check for radioactivity incorporation is then kept reasonable (10^4 – 10^6). It must be stressed that once a "cold colony" (which lacks radioactivity) has been found, roughly 10^4 mutant cells of the same genotype become available for further biological studies. With a 30×30 cm^2 MWPC, as we have tested, it would be possible to reconstruct in a single measurement a radioactivity map of $\sim 10^3$ colonies of the previously described topological distribution. Allowing one hour data taking to each measurement, we need 1000 h to scan 10^6 colonies, which is still a long time, but nothing exceptional compared with a standard biological experiment in this field.

As for the sensitivity of the chamber, it is necessary to estimate the counting rate per colony to be compared with the noise level. The most used β^- emitting radioisotopes in biological studies are shown in table 2, with some of the relevant parameters to this experiment, i.e. half-life, end-point energy of the β^- spectrum and "maximum range"; the latter has been calculated by means of empirical relationships [16].

^{35}S is commonly used for protein labelling and ^{32}P both for DNA and RNA nucleic acids; these two radioisotopes cannot be used in our experiment, i.e. to label the thymine, that contains neither S nor P atoms. On the other hand, the "maximum range" of the ^3H β^- spectrum is about 4 μm in Mylar (or few mm in air STP). In practice none of the elec-

Table 2
Relevant parameters of the most used β^- emitting radioisotopes in biological studies

	^3H	^{14}C	^{35}S	^{32}P
Half-life	12.26 y	5.73×10^3 y	66 d	14.3 d
Endpoint energy of the β^- spectrum (KeV)	18.6	156	167	1.71×10^3
"Maximum range" (mg/cm^2)	0.59	28.26	31.54	790.2

trons from ^3H decay would enter the active region of the chamber, unless the biological sample is positioned inside. Such a solution, which has been adopted in radiochromatography studies (17,18), would require a more complex mechanics and, most of all, would not ensure the survival of the cells during the measurement. Thus ^{14}C has been chosen.

If a 10 μm Mylar entrance window is used, with an additional 1 cm of air between the biological sample and the chamber and 0.2 cm of gas (argon/isobutane) before the active region of the MWPC, one obtains a total equivalent thickness of ~ 2.4 mg/cm^2 . By taking into account the corresponding transmission factor of the β^- spectrum, the solid angle acceptance and the detection efficiency of the chamber itself, one may estimate that about 30% of the β^- rays will be detected by the chamber.

The activity of each colony labelled with ^{14}C -thymidine, measured by means of liquid organic scintillator technique, is typically 150 disintegrations per minute [15]. In the experimental situation, with a density of colonies of about 1 colony/ cm^2 , the MWPC must detect an "effective" distribution of radioactivity of 10–100 pCi/ cm^2 . Similar or higher sensitivity has already been obtained [17,18]. From the measurements made on our prototype, we are confident that the electronic noise may be kept as low as 1 pCi/ cm^2 at a threshold level which does not impair too much the detection efficiency of the β^- .

We may then conclude that the real use of the MWPC in the proposed biological experiment will simply require an optimization of the chamber in terms of the dimension of the active volume (anode-cathode gap) and of the absorbers thickness (Mylar window, not active gas region, etc.), both for improving spatial resolution and increasing sensitivity. An optimized chamber in this respect is now being assembled.

6. Concluding remarks

In this paper we have shown that a MWPC with a cathode coupled delay line read-out can fulfill the spatial resolution, high sensitivity and low time consumption requirements for the biological problem under investigation, i.e. to isolate DNA repair deficient mutants in cultured mammalian cells. It is worth noticing that such a non-destructive method for radioactivity counting of living cells may prove to be of practical value in many other cases when

variations in the ability of cell clones and other cell aggregations to incorporate or attract radioactivity precursors have to be studied. Tracers are nowadays used in many fields of experimental biology, from biochemistry to molecular biology, genetics, immunology, to recall only a few. Several other applications may then be envisaged for this kind of detector (19,20), which may contribute towards the solution of highly relevant problems in biomedical sciences.

It is a pleasure to thank the Director of INFN Sezione di Pisa, Prof. A. Stefanini, for his continuous support and encouragement in this work and Dr. A. Abbondandolo (CNR Institute of Mutagenesi e Differenziamento di Pisa) for many useful discussions. Messr M. Giardoni and M. Del Colletto have been of much help in the construction of the chamber; many thanks are due to Mr. A. Bechini for his enthusiasm and skill during the setting-up of the experimental apparatus.

References

- [1] J.E. Cleaver, *Nature* 218 (1968) 652.
- [2] J.E. Cleaver, in *Progress in genetic toxicology*, eds., D. Scott, B.A. Bridges and F.H. Sobels (Elsevier, Amsterdam, 1977) p. 29.
- [3] J.E. Cleaver, in *Handbook of mutagenicity test procedures*, eds., B.J. Kilbey, M. Legator, W. Nichols and C. Ramel (Elsevier, Amsterdam, 1977) p. 19.
- [4] A. Abbondandolo, S. Bonatti, C. Colella, G. Corti, F. Matteucci, A. Mazzaccaro and G. Rainaldi, *Mutation Res.*, 37 (1976) 293.
- [5] J.E. Cleaver, *Radiation Res.*, 37 (1969) 334.
- [6] G. Charpak, R. Bouclier, T. Bressani, J. Favier and C. Zupančič, *Nucl. Instr. and Meth.* 62 (1968) 235.
- [7] G. Charpak, D. Rahm and H. Steiner, *Nucl. Instr. and Meth.* 80 (1970) 13.
- [8] G. Charpak and F. Sauli, CERN report 73/4 (1973).
- [9] J.L. Lacy and R.S. Lindsey, *Nucl. Instr. and Meth.* 119 (1974) 483.
- [10] R. Grove, K. Lee, V. Perez-Mendez and J. Sperinde, *Nucl. Instr. and Meth.* 89 (1970) 257.
- [11] V. Perez-Mendez, M. Greenstein and D. Ortendahl, *IEEE Trans. Nucl. Sci.* NS24 (1977) 209.
- [12] H.E. Kallmann, *Proc. I.R.E.* 34 (1946) 646.
- [13] M.O. Bedwell and J.J. Paulus, *IEEE Trans. Nucl. Sci.* NS26 (1979) 422.
- [14] H. Okuno, R.L. Chase, J. Fisher and A.H. Walenta, *IEEE Trans. Nucl. Sci.* NS24 (1977) 213.
- [15] A. Abbondandolo, private communication.
- [16] R.D. Evans, *The atomic nucleus* (McGraw-Hill, New York, 1967) p. 625.

- [17] Yu. V. Zanevsky, S.P. Chernenko, A.B. Ivanov, L.B. Kamini, V.D. Peshekhonov, E.P. Senchenkov, I.A. Tyapkin and V.N. Kalinin, *Nucl. Instr. and Meth.* 153 (1978) 445.
- [18] Yu. Anisimov, S.P. Chernenko, A.B. Ivanov, V.N. Kalinin, V.D. Peshekhonov, E.P. Senchenkov, I.A. Tyapkin and Yu. V. Zanevsky, *J. Chromatogr.* 178 (1979) 117.
- [19] Proc. of Wire Chamber Conference, Wien, Austria, February 14–16, 1978, eds., W. Bartl and M. Regler, *Nucl. Instr. and Meth.* 156 (1978) 1–71.
- [20] Proc. of Wire Chamber Conference, Wien, Austria, February 27–29, 1980, eds., W. Bartl and M. Regler, *Nucl. Instr. and Meth.* 176 (1980) 67–117.